Case Study

Video-rate Two-photon Microscopy to Take a Closer Look at Chloride Homeostasis in Mice Carrying AD-linked Mutations

BliQ PHOTONICS

Cover image reference: *Courtesy of Lionel Froux and Iason Keramidis, Dr. Antoine Godin's lab, CERVO Research Centre, Laval University.*

CASE STUDY

Video-rate Two-photon Microscopy to Take a Closer Look at Chloride Homeostasis in Mice Carrying AD-linked Mutations

Bliq Photonics manufactures a Multiphoton Video-rate Microscope System (VMS) that features a high-speed polygonal scanner capable of supporting rates of acquisition from 32 to 900 fps (1024×512 and 1024×8, respectively) with precise control of pixel dwell time across the entire field of view (**Fig. 1**). This, combined with the stability and flexibility offered by its reduced system complexity, allows VMS to support a wide range of imaging applications to study biological events in living tissues.

In their publication: Restoring Neuronal Chloride Extrusion Reverses Cognitive Decline Linked to Alzheimer's Disease Mutations, Dr. Iason Keramidis (from the laboratory of Dr. Yves De Koninck at CERVO Research Centre, Laval University) and colleagues have leveraged these attributes of VMS to gain a unique insight into the neurobiological underpinnings of Alzheimer's disease (AD). It has been postulated that disinhibition through disrupted GABAA-mediated inhibitory signaling during the early stages of AD causes network dysfunction and hyperexcitability, leading to cognitive deficits. The neuronal membrane potassium-chloride cotransporter KCC2 is responsible for maintaining a low intracellular chloride concentration ([Cl-]i) in neurons by extruding chloride, preserving the robustness of GABAA-mediated inhibition. Interestingly, there is both clinical (Doshina et al., 2017) and experimental (Bie et al., 2022) evidence that KCC2 expression is reduced in AD. Given this, the team hypothesized that KCC2 hypofunction underlies cognitive deficits in mice carrying AD-linked mutations that result in Aβ pathology. They address this possibility through a series of experiments that included a collaborative initiative with the laboratory of Dr. Antoine Godin to quantitatively assess chloride homeostasis in individual neurons that express the Fluorescence Resonance Energy Transfer (FRET)-based chloride sensor, SuperClomeleon (**Fig. 2**).

To test for deficits in neuronal chloride extrusion capacity, ex vivo chloride imaging was performed in mice that received AAV2/9.CaMKIIa.SuperClomeleon injections in the medial prefrontal cortex (mPFC) and hippocampal CA1 region at 4 and 6 months of age, respectively. 4 weeks after viral injection, imaging work in brain slices was divided between a confocal laser-scanning microscope and the VMS - both coupled to a fluorescence lifetime imaging (Becker and Hickl GmbH) module. In response to a stepped extracellular K+ ([K+]e) from 5 to 15 mM (**Fig. 3B and E**) to reverse Cl- transport through the KCC2 transporter, fluorescence lifetime measurements of Cl- revealed that the rate of Cl- accumulation was significantly slower in the mPFC and CA1 (**Fig. 3C and F, respectively, right panels**) of 5xFAD mice with AD-related mutations compared to age-matched control Non-Transgenic (Non-Tg) mice, reflecting weaker Cl- transport capacity in the 5xFAD mice. Essential to this interpretation, the investigators were able to take advantage of the rapid and reliable volumetric imaging capability of the VMS through successive Z-stacks of a large region of interest in CA1 during a K+ extracellular challenge (from 5 to 15 mM) and found that there was no difference in neuron diameters following the increase in [K+]e (**Supplementary Figure 7**), indicating that the observed [Cl-]i changes were not secondary to a change in cell volume.

CASE STUDY

Video-rate Two-photon Microscopy to Take a Closer Look at Chloride Homeostasis in Mice Carrying AD-linked Mutations

To ensure the difference measured in brain slices was not due to an effect of the preparation, the VMS also enabled the group to follow up with in vivo chloride imaging. These experiments were performed in mice prepared in an analogous manner to the above but focused on the mPFC. Anesthetized 4-month-old mice with a cranial window prepared over the PFC were head-fixed under the VMS (**Fig. 3G, left panel**). With appropriate filters in place on the VMS, it was possible to concurrently monitor YFP (acceptor) and CFP (donor) signal intensity in separate channels (**Fig. 3G, right panel**). Ratiometric measurements of intracellular chloride concentration (**Fig. 3H**) revealed that the median FRET ratio of pyramidal neurons from 5xFAD mice with AD-related mutations was significantly lower than NonTg neurons, indicating higher [Cl-]i (**Fig. 3I, left panel**).

The impairment of chloride homeostasis observed in the above imaging experiments coincides with the downregulation of KCC2 in the mPFC and CA1 of 5xFAD mice (see Keramidis et al. (2023) for further details). Given this consistency, they further assessed the possibility of KCC2 hypofunction through additional experiments with the KCC2 enhancer, CLP290. Here, fluorescence lifetime imaging in brain slices with the VMS revealed that CLP290 treatment restored the rate of Cl- accumulation evoked by the rise in [K+]e in CA1 neurons from 5xFAD mice (**Fig. 4C-E**). CLP290 also protected against deterioration of learning and cortical hyperactivity (see Keramidis et al. (2023) for further details), and therefore these findings collectively point to KCC2 hypofunction as a viable target that can inspire future therapeutic interventions in the treatment of AD.

CASE STUDY

VIDEO-RATE TWO-PHOTON MICROSCOPY TO TAKE A CLOSER LOOK AT CHLORIDE HOMEOSTASIS IN MICE CARRYING AD-LINKED MUTATIONS

FIGURES AND LEGENDS

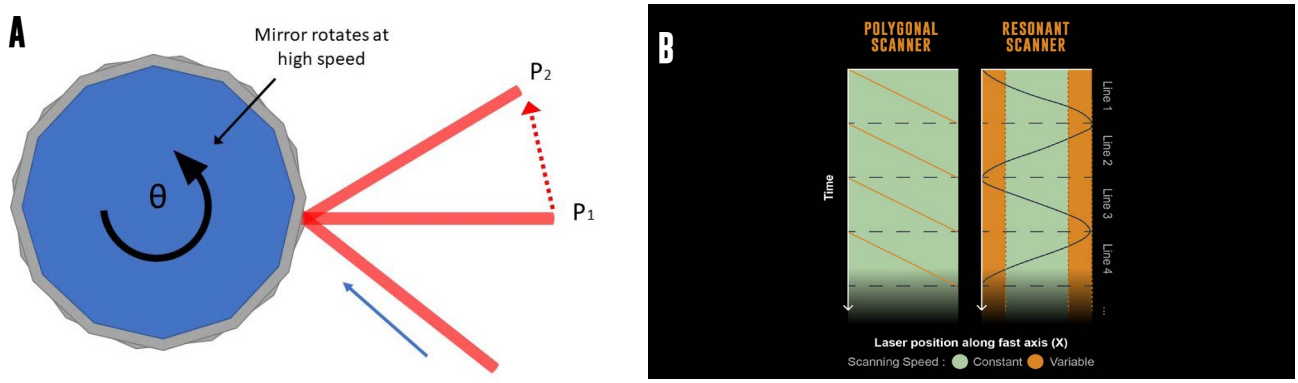

Figure 1. Polygonal scanner rotation and linearity. (A) A polygonal scanning mirror rotates around a center point (left panel), sweeping the beam position (red bar) from P1 to P2. (B) Unlike a resonant scanner (right), the constant speed of the polygonal scanner (left) provides linearity, resulting in precise control over time spent at each pixel (dwell time) across the entire field of view. Illustration in (A) adapted from Colarusso and Brideau (2023).

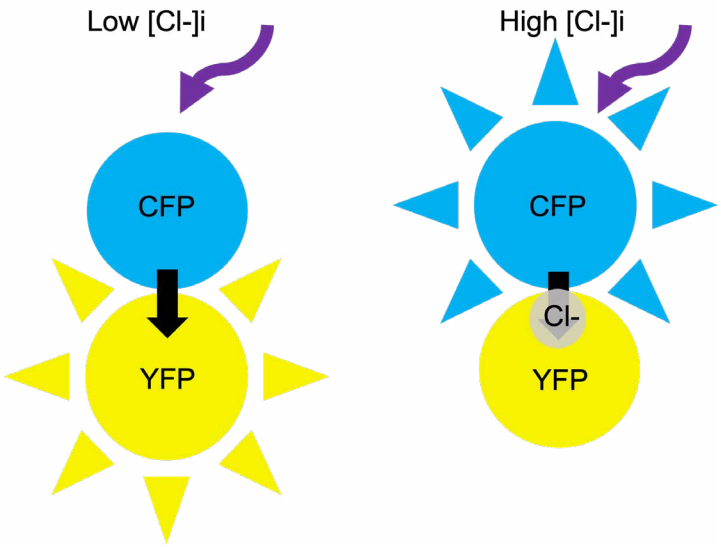

Figure 2. SuperClomeleon is a FRET-based chloride sensor. CFP (donor, blue) and YFP (acceptor, yellow) relative signal in low [Cl-]i (left) and high [Cl-]i (right) upon excitation (purple arrows). Chloride quenching of the acceptor (gray circle) disrupts FRET activity (black arrows) and decreases the FRET Ratio (acceptor channel/donor channel). Adapted from Herstel et al. (2022).

CASE STUDY

Video-rate Two-photon Microscopy to Take a Closer Look at Chloride Homeostasis in Mice Carrying AD-linked Mutations

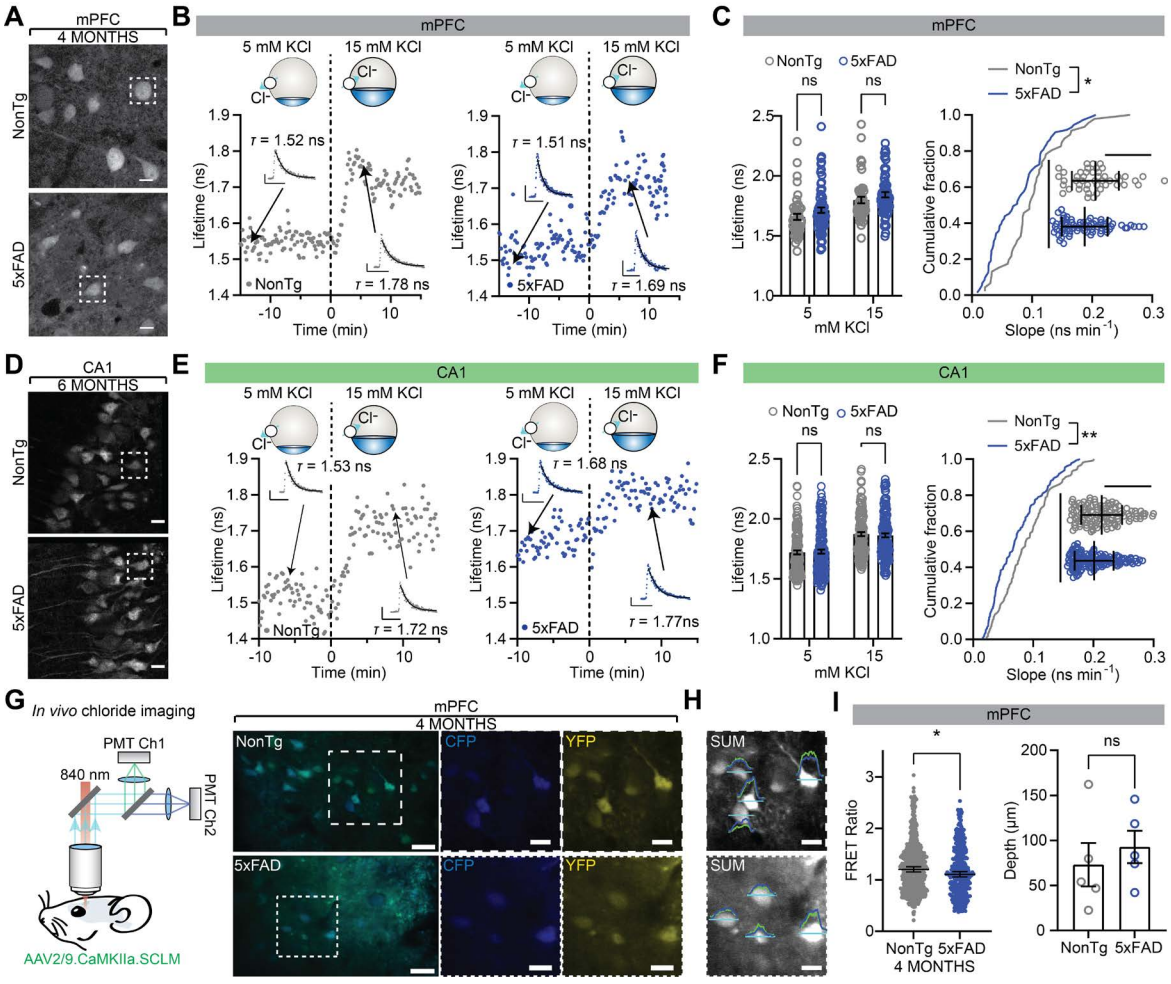

Figure 3. Impaired chloride transport in 5xFAD mice. (A and D) FLIM images of 5xFAD and NonTg CaMKIIa-positive neurons expressing SuperClomeleon in mPFC (A) and hippocampal (D) slices (Scale bars: 10 µm). (B) Timelapse recording of Cl- accumulation in the cell body of selected NonTg (gray) and 5xFAD (blue) neurons from the ROI in A upon 15 mM KCl extracellular application (dashed line). Insets show examples of fitted photon-distribution histograms during the low KCl condition (left) and upon 15 mM KCl application (right). Scale bars: vertical, 50 photons; horizontal, 5 ns. (C) The mean lifetime of NonTg and 5xFAD neurons during the baseline condition (5 mM KCl) and upon 15 mM KCl application. The distribution of the mean rate of Cl- changes measured in 4-month-old 5xFAD and NonTg mPFC slices. The inset presents the mean slope (± SD) measured in individual neurons from 5xFAD and NonTg mice (Scale bar: 0.1 ns min-1; 5xFAD: n = 73 neurons from N = 10 mice; NonTg: n = 46 neurons from N = 7 mice).

VIDEO-RATE TWO-PHOTON MICROSCOPY TO TAKE A CLOSER LOOK AT CHLORIDE HOMEOSTASIS IN MICE CARRYING AD-LINKED MUTATIONS

(E) Similar to B but for NonTg and 5xFAD CA1 neurons within ROIs shown in D. (F) Similar to C but for CA1 neurons from 6-month-old 5xFAD and NonTg mice (Scale bar: 0.1 ns min-1; 5xFAD: n = 133 neurons from N = 6 mice; NonTg: n = 122 neurons from N = 5 mice). (G) Graphical illustration of the SuperClomeleon in vivo steady state imaging experimental setup, and representative images of the mean intensity of YFP and Cerulean merged (left) and split for the areas selected in dashed squares (right) in the prefrontal cortex of 4-month-old 5xFAD and NonTg mice (Scale bars: 20 µm and 10 µm for the selected areas). (H) Images of the sum of the CFP and YFP fluorescence intensity of the selected areas in G and intensity profiles of CFP (blue) and YFP (green) for the lines in cyan. (I) The median FRET ratio of 5xFAD vs. NonTg neurons (left; 5xFAD: n = 361 neurons from N = 5 mice; NonTg: n = 638 neurons from N = 5 mice) and the estimated mean depth of imaging (right; Mean ± SEM). * P < 0.05; *** P < 0.001; ns = non-significant.

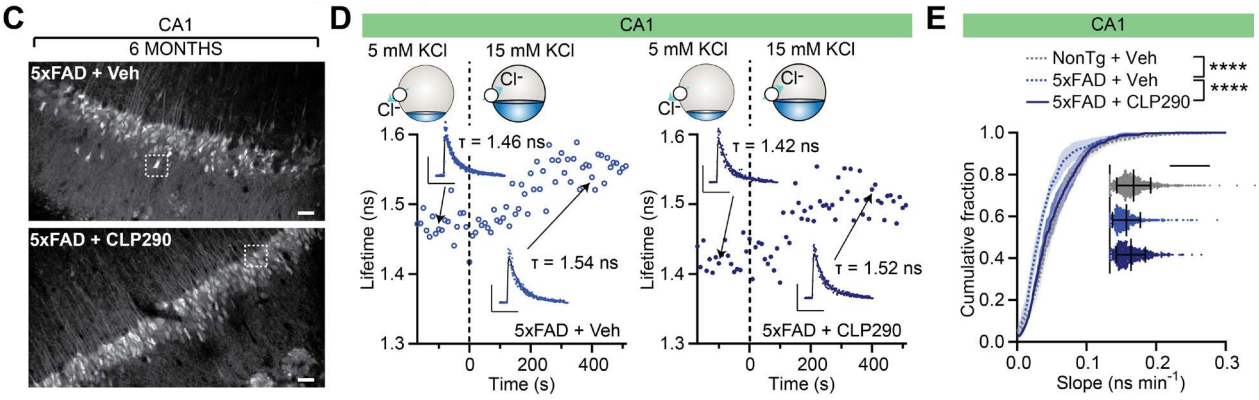

Figure 4. CLP290 restores chloride transport in 5xFAD mice. (C) FLIM images of CaMKII-positive neurons expressing SuperClomeleon in the CA1 of vehicle- and CLP290-treated 5xFAD mice (Scale bars: 25 µm). (D) Timelapse recording of Cl- accumulation in the cell body of selected vehicle-treated 5xFAD (blue circles) and CLP290-treated 5xFAD (dark blue dots) neurons from the ROI in C upon 15 mM KCl extracellular application (dashed line). Insets show examples of fitted photon-distribution histograms during the low KCl condition (left) and upon 15 mM KCl application (right). Scale bars: vertical, 100 photons; horizontal, 4.8 ns. (E) Distribution of the average rate of Cl- changes (slope) measured in the CA1 of 6-month old CLP290-treated 5xFAD mice and vehicle-treated 5xFAD and NonTg mice. Inset displays the mean slope (± SD) measured in individual neurons from CLP290-treated 5xFAD mice and vehicle-treated 5xFAD and NonTg mice (Scale bar: 0.1 ns min-1; NonTg + Veh: n = 1028 neurons from N = 6 mice; 5xFAD + Veh: n = 639 neurons from N = 4 mice; 5xFAD + CLP290: n = 675 neurons from N = 6 mice). * P < 0.05; ** P < 0.01; **** P < 0.0001; ns = non-significant. Adapted from Keramidis et al. (2023).

CASE STUDY

Video-rate Two-photon Microscopy to Take a Closer Look at Chloride Homeostasis in Mice Carrying AD-linked Mutations

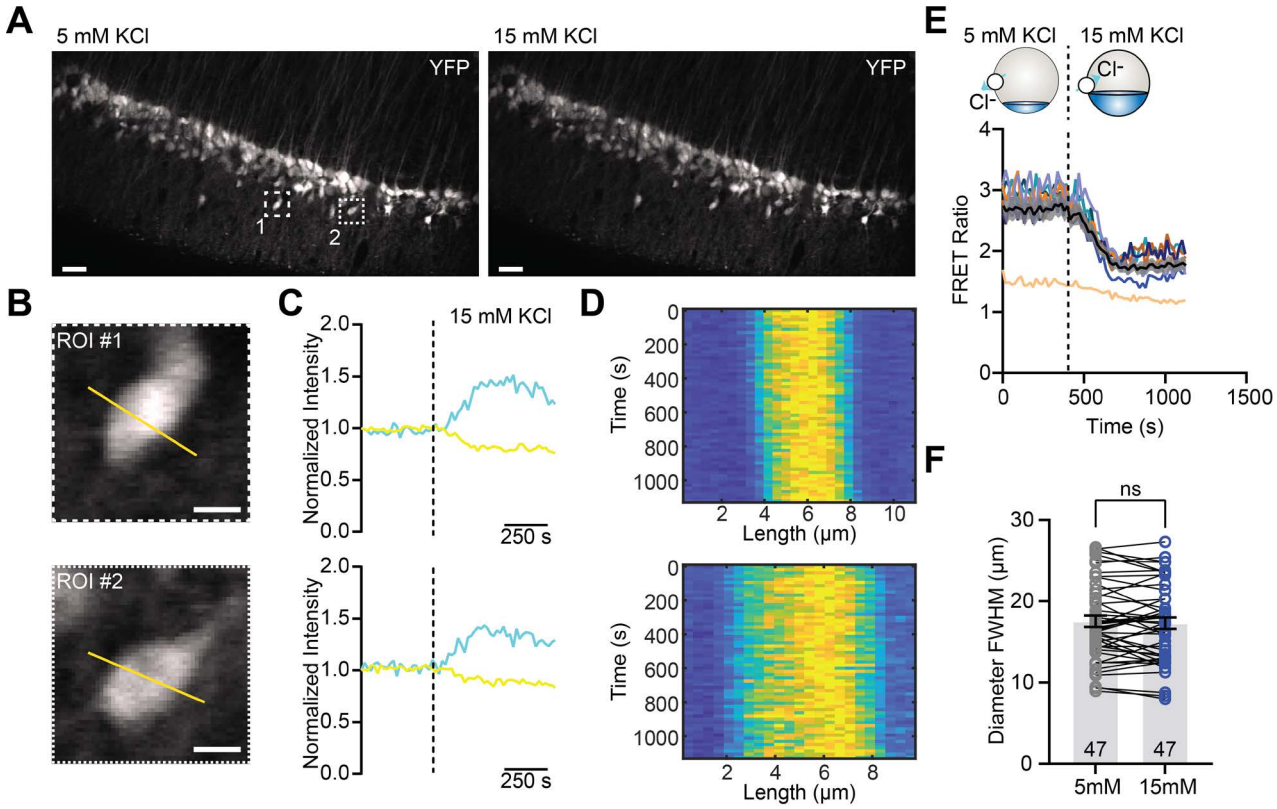

Supplemental Figure 7. Neuron cell body diameter is unaltered after stepping extracellular K+ from 5 to 15 mM. (A) Two-photon images of the green fluorescence channel (Chroma ET530/30x) of CaMKIIapositive CA1 hippocampal neurons transduced with SuperClomeleon in two different conditions. Left: the slices in ASCF with low extracellular KCl (5 mM). Right: the same slice in ACSF with high extracellular KCl (15 mM). Scale bar 25 µm. (B) Neurons from selected ROIs in A (Scale bar 5 µm). The yellow dissecting lines were used to calculate the fluorescence intensity profile at each time point of the kymographs in D. (C) Normalized fluorescence intensity of CFP (cyan) and YFP (yellow) across time for the neurons selected in the ROIs. The dashed line represents the time point when the extracellular solution was changed to ASCF with 15 mM KCl. (D) Kymograph presenting the intensity profile along the yellow line shown in B as a function of time. Each line was used to estimate the cell body diameter using the full width at half maximum (FWHM) of each intensity profile. (E) Timelapse measurement of the intensity FRET ratio (green channel: Chroma ET530/30x; blue channel: Chroma ET473/24m) of all selected neurons from the temporal acquisition in A. The black line shows the mean FRET ratio ± SEM (n = 8 neurons). (F) The mean FWHM neuron diameter for the 5 mM and 15 mM KCl ASCF conditions (n = 47 neurons from N = 5 slices). ns = non-significant (paired t-test).

REFERENCES

Keramidis I, McAllister BB, Bourbonnais J et al. Restoring neuronal chloride extrusion reverses cognitive decline linked to Alzheimer's disease mutations. Brain. 2023. doi:10.1093/brain/awad250. Online ahead of print.

Doshina A, Gourgue F, Onizuka M, et al. Cortical cells reveal APP as a new player in the regulation of GABAergic neurotransmission. Sci Rep. 2017;7(1):370. doi:10.1038/s41598-017-00325-2

Bie B, Wu J, Lin F, Naguib M, Xu J. Suppression of hippocampal GABAergic transmission impairs memory in rodent models of Alzheimer's disease. Eur J Pharmacol. 2022;917:174771. doi:10.1016/J.EJPHAR.2022.174771

Herstel LJ, Peerboom C, Uijtewaal S, et al. Using SuperClomeleon to measure changes in intracellular chloride during development and after early life stress. eNeuro. 2022;9(6). eNeuro. doi:10.1523/ENEURO.0416-22.2022

Colarusso P and Brideau C. Speed running your sample: faster laser scanning in confocal and multiphoton microscopes. March 22, 2023. Bliq Photonics. https://bliqphotonics.com/faster-laser-scanning-confocal-multiphoton-microscopes/

Bliq Photonics is a Canadian company founded and based in Quebec City, that designs and manufactures imaging systems for life science applications. Our growing portfolio, backed by patented technologies, supports a variety of experiments. Our technologies include multiphoton, real-time volumetric imaging, confocal and light sheet systems.

Bliq's team understands customer vision, and crafts each imaging and multiphoton solution to meet high standards of usability and reliability.

Fueled by many years of microscopy experience we know that support and collaboration begins with a commitment to each customer.

Why not experience Bliq today?

CONTACT US

CONTACT US

1.844.629.5413

info@bliqphotonics.com

OFFICES

1405 Boul. du Parc technologique
2nd floor
Quebec City, QC
Canada, G1P 4P5

LABORATORIES

2601 Chemin de la Canardière
Suite F-4434
Quebec City, QC
Canada, G1J 2G3